ICELL JOURNAL | RESEARCH ARTICLE

Articles

Resveratrol Oligomers Trans-gnetin H Promotes Reactive Oxygen Species Generation and Rictor Degradation to Suppress Cancer Cell Viability

DOI:https://doi.org/10.71373/UGHK9221
Submitted 27 June 2025
Accepted 12 August 2025
Published 26 August 2025

Shiyang Lou[a,1], Ruixu Zhang [a,1], Chao Xia[a,1], Yining Zheng[a], Miaomiao Zhu[a], Dingping Feng[a], Lu Deng[a,b*]

The function of resveratrol as an antioxidant is to scavenge reactive oxygen species (ROS) in the body. The effects of resveratrol on cell ular activity have been widely reported. Trans-gnetin H is a trimer of resveratrol that is found in seeds of peonies. However, there is n ot enough research on the cellular effects of trans-gnetin H, and it is not clear if it has the same physiological functions as resveratrol. This study tries to answer this question by investigating the effect of trans-gnetin H on ROS, mammalian target of rapamycin (mTOR), c ell viability, autophagy, and ferroptosis in several cancer cell lines. Trans-gnetin H was found to regulate cell viability, cell proliferation, and autophagy, but it did not affect ferroptosis. Molecular experiments showed that these effects were brought about via significant promotion of ROS generation and suppression of mTOR activation in an ROS-dependent manner. Further mechanistic experiments sho wed that trans-gnetin H inhibits mTOR activation by inducing FBXW7-mediated ubiquitination and degradation of Rictor, a key compon ent of mTORC2. Thus, trans-gnetin H appears to control tumor cell viability by inhibiting activation of the mTORC1 and mTORC2 pathw ays through a novel regulatory mechanism involving the ROS-Rictor signaling axis.

1.Introduction

Reactive oxygen species (ROS) are commonly found in the for m of molecular oxygen derivatives such as O2- and H2O2. Th ere are many sources of intracellular ROS, which can be gene rated in the plasma membrane, cytoplasm, and organelles (in cluding the endoplasmic reticulum, mitochondria, and peroxi somes) [1]. ROS production and ROS elimination need to be b alanced for the maintenance of the intracellular redox state and several cell-, organ-, and organism-level physiological pr ocesses such as formation of the extracellular matrix, wound healing, and immunity [2-4]. ROS accumulation can lead to v arious diseases, including cancer, by inducing oxidative dama ge to proteins, DNA, and lipids. Interestingly, excessive ROS l evels may also cause tumor cell death. Therefore, the target of numerous chemotherapeutic methods for the treatment o f tumors is ROS-induced cell death. As a result, there is consi derable ongoing research about the mechanisms associated with ROS-induced cell death and related treatment targets th at could be applied in cancer therapy.

Resveratrol is a commonly found polyphenolic compound wit h known antioxidant, anti-inflammatory, and immunomodula tory properties, among other benefits. Resveratrol has a broa d spectrum of anti-tumor effects, showing significant anti-tu mor activity in a variety of tumor cells. It can inhibit the grow th, proliferation, invasion and metastasis of cancer cells thro ugh a variety of signaling pathways and regulate the expressi on of related proteins, induce cell apoptosis, and reverse che motherapy resistance and enhance chemotherapy sensitivity. Trans-gnetin H [5] is a natural polyphenolic compound that i s structurally composed of a trimer of resveratrol and one of the most important stilbenes in peony seeds. There is a large body of literature on the antitumor effects and mechanisms of resveratrol, but studies on the antitumor activity and mec hanisms of trans-gnetin H are few. In our previous study, we reported the antitumor potential of trans-gnetin H[6] and fo und that trans-gnetin H controls tumor cell growth through r egulation of autophagy [5]. In line with this observation, it is known that resveratrol, the compound that forms trans-gneti n H, plays a role in the initiation of autophagy [7-9]. In additi on, the antioxidant activity of resveratrol is one of its main fu nctions[10-13], and it is also known to be involved in the ind uction of apoptosis [9, 14, 15] and cell necrosis [16]. In contr ast to these findings for resveratrol, the results of our previo us study indicated that trans-gnetin H did not play a role in re gulating apoptosis [5]. Further, it is not clear whether trans-g netin H has antioxidant capacity. Thus, although trans-gnetin H is composed of resveratrol, it does not possess all the char acteristics of resveratrol.

In our previous study, we also discovered that trans-gnetin H regulates autophagy via the mammalian target of rapamycin (mTOR) complex 1 (mTORC1) pathway. mTOR is an atypical s erine/threonine protein kinase that integrates a variety of ex tracellular signals, including amino acids, glucose, lipids, gro wth factors, and ROS, and is essential for autophagy [17]. It is primarily found in two intracellular complexes—mTORC1 an d mTORC2—which are sensitive and respond to different sig nals (including ROS) and, thus, exert different functions [18]. In our previous study, even though we discovered that trans-gnetin H can regulate the mTORC1 pathway, it was unclear w hether it affects the mTORC2 pathway. In the present study, we have tried to gain a better understanding of the antitumo r activity and mechanisms of trans-gnetin H by investigating i

a College of Animal Science and Technology, Northwest A&F University, Yangling, Shanxi 712100, China;
b Shenzhen Research Institute, Northwest A&F University, Shenzhen, Gu angdong, 518000, China;
1 These authors contributed equally to this article;
* Corresponding author
denglu128128@nwafu.edu.cn (L. Deng)
Running title: Trans-gnetin H Suppress Cancer Cell Viability

ts effects on ROS levels and the mTOR pathway in several cancer cell lines. We believe that these findings will shed light on the functions of trans-gnetin H and the underlying autophagy-related mechanisms in tumor cells and also help identify potential therapeutic targets for antitumor treatment.

2. Materials and methods

2.1 Materials

Erastin (E7781), RSL3 (SML2234), cycloheximide (CHX), N-acetylcysteine (NAC, A7250), dichlorofluorescein diacetate (DCFH-DA, 35845), and secondary antibodies were obtained from Sigma-Aldrich (MO, USA). Antibodies for pT389-S6K (9234S/L), S6K (9202S), Rictor (9476), pS473-AKT (9271), AKT (9272), and SOD1 (37385) were obtained from Cell Signaling Technology (MA, USA). Actin (20536-1-AP), FBXW7α (28424-1-AP), Nrf2 (16396-1-AP), and HMOX1 (10701-1-AP) were obtained from Proteintech (Chicago, USA). NQO1 (ab80588) was obtained from Abcam (Cambridge, UK). β-mercaptoethanol, penicillin, fetal bovine serum (FBS) and streptomycin were purchased from Gibco (Grand Island, NY, USA). Phosphate-buffered saline (PBS) and trypsin were purchased from HyClone (UT, USA). Trizol reagent, the PrimeScript RT reagent kit (RR047A), and the TB Green quantitative real-time quantitative polymerase chain reaction (qRT-PCR) kit (RR820A) were purchased from Takara (Dalian, China). Cell counting kit-8 (CCK8, K009) was purchased from ZETA LIFE (CA, USA). BODIPY 581/591 C11 (D3861) was purchased from Thermo Fisher Scientific (MA, USA).

2.2 Origin and purity of trans-gnetin H

Trans-gnetin H (purity, >99%) was obtained from the seeds of the tree peony. For the cellular experiments, trans-gnetin H was dissolved in dimethyl sulfoxide to the required concentrations. The extraction and isolation of trans-gnetin H was conducted according to the published protocol [19]. Structural determination of isolated trans-gnetin H was elucidated by 1H- and 13C-NMR as below:

1H-NMR (500 MHz, CD3OD)δ (ppm): 7.19 [4H,dd, J = 2.0, 8.5 Hz, H-2(6), 2″ (6″)], 6.79 [4H, dd, J = 2.0,8.5 Hz, H-3(5), 3″ (5″)], 6.69 (2H, d, J = 8.5 Hz, H-2′, 6′),6.51 (2H, d, J = 8.5 Hz, H-3′, 5′), 6.43 (1H, s, J = 8.5 Hz,H-12), 6.39 (2H, s, H-7′, 8′), 6.15 [6H, s, H-10(10″),12(12″), 14(14″)], 5.41 (2H, d, J = 5.5 Hz, H-7, 7″), 4.41(2H, d, J = 5.5 Hz, H-8, 8″).

13C-NMR (125 MHz, CD3OD)δ (ppm):163.5 (C-11′, 13′), 160.6 [C-11(11″), 13(13″)],159.0 (C-4, 4″), 158.8 (C-4′), 148.0 (C-9, 9″), 135.0 (C-9′),134.6 (C-1″), 134.2 (C-1), 131.1 (C-1′), 129.14 (C-2′, 6′,8′), 128.6 [C-2(2″), 6(6″)], 123.0 (C-7′), 120.8 (C-10′, 14′),116.8 [C-3(3″), 5(5″)], 116.6 (C-3′, 5′), 107.8 [C-10(10″),14(14″)], 102.6 (C-12, 12″), 95.3 (C-7, 7″), 91.9 (C-12′),59.4 (C-8, 8″).

The 1H- and 13C-NMR of trans-gnetin H only used for review because our related work haven't been published.

The purity of trans-gnetin H was confirmed using HPLC. Evidence is presented in the supplementary material of our previously published articles.

2.3 Cell culture

HT29, H1299, MDA231, and HepG2 cells were purchased from National Science & Technology Infrastructure (NSTI, Shanghai, China) and cultured according to the manufacturer's protocol. HT29 and H1299 cells were cultured in RPMI 1640 medium (Hyclone, USA), MDA231 and HepG2 cells were cultured in Dulbecco's modified Eagle medium (DMEM; Hyclone, USA) containing 10% FBS (Gibco, Grand Island, NY, USA) according to the ATCC guidelines.

2.4 Sample collection and preparation for lipidomic analysis

HT29 cells were treated with 10 μM trans-gnetin H for 2 hours. Cells from both control and trans-gnetin H-treated groups were then harvested. Six replicate samples per group (each contains 1 ×107 cells precisely counted via Cytometer, BioRad, Hercules, USA) were flash-frozen in liquid nitrogen and stored at -80°C for lipid extraction and LC-MS analysis. Lipids were extracted following Matyash [20] with modifications. Briefly, samples were thawed at 4°C before adding 200 μL ice-cold distilled water. Homogenization was performed with 240 μL ice-cold methanol, followed by vortexing. After adding 800 μL methyl tert-butyl ether (MTBE), samples were vortexed, sonicated in an ice-water bath for 20 min, then incubated at room temperature for 30 min. Following centrifugation (14,000 × g, 15 min, 10°C), the upper organic phase was collected and dried under nitrogen. For LC-MS analysis, dried lipids were reconstituted in 200 μL isopropanol, vortexed, centrifuged (14,000 × g, 15 min, 10°C), and the supernatant collected. A pooled quality control (QC) sample was generated by combining equal aliquots from each lipid extract.

2.5 LC-MS/MS analysis for lipids

Lipidomic analysis was performed according to the methods [21,22]. Briefly, samples were maintained at 10°C in an autosampler, with 3 μL aliquots injected onto a reverse-phase CSH C18 column (Waters ACQUITY UPLC CSH C18; 1.7 μm, 2.1 × 100 mm) via a UPLC system (SHIMADZU, Japan). The mobile phase comprised Solvent A (acetonitrile–water, 6:4 v/v, 0.1% formic acid, 0.1 mM ammonium formate) and Solvent B (acetonitrile–isopropanol, 1:9 v/v, 0.1% formic acid, 0.1 mM ammonium formate), with a gradient starting at 30% Solvent B (300 μL/min), held for 2 min, linearly increased to 100% Solvent B over 23 min, and equilibrated at 5% Solvent B for 10 min. Sample order was randomized to mitigate instrumentation bias. Post-separation, mass spectrometry was conducted on a Q-Exactive Plus (Thermo Scientific, USA) with shared parameters (heater 300°C, sheath gas 45 arb, auxiliary gas 15 arb, sweep gas 1 arb, capillary 350°C); For positive (ESI+) used 3.0 kV

spray voltage, S-Lens RF 50%, and MS1 scan 200–1800 m/z, while for positive (ESI−) used 2.5 kV, S-Lens RF 60%, and MS2 scan 250–1800 m/z. Quality control samples were analyzed at each batch start and after every 5 samples to ensure data stability.

Raw data were processed using LipidSearch™ Software (v4.1, Thermo Fisher Scientific, CA, USA) for peak alignment, retention time correction, and peak area quantification. Analytical method validation was performed with key parameters set as follows: precursor tolerance = 5 ppm, product tolerance = 5 ppm, and product ion threshold = 5%. Lipid species exhibiting >30% relative standard deviation (RSD) or >50% missing values were excluded from the LipidSearch-extracted dataset. Following normalization and integration via Pareto scaling, processed data were subjected to principal component analysis (PCA) using SIMCA-P® software (v14.1, Umetrics, Umea, Sweden). Identified metabolites were annotated against the KEGG pathway database (https://www.genome.jp/kegg/pathway.html). Volcano plots were subsequently generated using R software.

2.6 siRNA knockdown

Non-specific control siRNA and siRNAs for FBXW7α were purchased from GenePharma (Shanghai, China). Transfection of cells with the siRNA oligonucleotides was performed using Lipofectamine 2000 (Invitrogen, CA, USA) according to the manufacturer's instructions. The siRNAs used are listed here:

si NC：5'-UUCUCCGAACGUGUCACGU-3'

si FBXW7α-1: 5'-GCTCCCTAAAGAGTTGGCACTCTAT-3'

si FBXW7α-2：5'-ACAGGACAGUGUUUACAAATT-3'

2.7 Western blot analysis

The western blotting protocol used has been described by us previously [23]. It can be briefly summarized as follows: the cells were washed with PBS, lysed with radio immune precipitation assay buffer for 30 min, and centrifuged at 12,000 rpm for 15 min (4oC). The supernatant was subjected to sodium dodecyl sulfate-polyacrylamide gel electrophoresis (SDS-PAGE) for separation of proteins, and the proteins were transferred to nitrocellulose (NC) membranes (0.45 µm, GE). The NC membranes were then blocked with non-fat milk and incubated with primary antibodies overnight at 4°C. Next, the membranes were washed with PBS and incubated with secondary antibodies (containing horseradish peroxidase) for 1–2 h. Following this, the membranes were washed with PBST, and the target proteins were detected with an imaging system from Bio-Rad (Hercules, CA, USA). Protein abundance was quantified using the ImageJ software.

2.8 Quantitative qRT-PCR analysis

Total RNA was isolated using TRIzol reagent and reverse transcribed with the PrimerScript RT reagent kit. qRT-PCR analysis was performed with the TB Green qRT-PCR kit. The comparative Ct method was used to determine the relative quantity of the mRNA of the target gene, with the GAPDH gene as the internal control. The sequences of the primer pairs used are shown in Table 1.

Table 1 Primer sequences for qRT-PCR

Gene	Forward primer sequence (5'→3')	Reverse primer sequence (5'→3')
HMOX1	TGCTCAACATCCAGCTCTTTGA	AACTGTCGCCACCAGAAAGC
SOD1	ACAAAGATGGTGTGGCCGAT	AACGACTTCCAGCGTTTCCT
NQO1	GAAGAGCACTGATCGTACTGGC	GGATACTGAAAGTTCGCAGGG
Rictor	CGAGTACGAGGGCGGAAT	ATCTGGCCACATTTTGGAGA
GAPDH	CAACGAATTTGGCTACAGCA	AGGGGTCTACATGGCAACTG

2.9 Detection of lipid ROS

Cells were seeded in 6-well plates or 24-well plates and were treated with trans-gnetin H for 24 h. The cells were then incubated with DCF-DA or 5 µM BODIPY C11 at 37°C for 30 min. The cells in the 6-well plates were washed, and fluorescence intensity was detected by flow cytometry (BD FACSAria III, USA).

2.10 Cell viability assay

For the determination of cell viability, cells were seeded in 96-well plates at a density of 104 cells/well and incubated with complete RPMI 1640 medium containing reagents. The medium was replaced with 100 µL fresh medium containing 10% CCK8 reagent, and this was followed by incubation for 3 h at 37°C. The plate was then read with a Synergy HT microplate reader (Bio-Tek, USA) (absorbance, 450 nm).

2.11 Colony formation assay

Cells were seeded in 6-well plates at a density of 1000–2000 cells/well and treated with different combinations of regents. This was followed by culture in RPMI-1640 medium containing 10% FBS for 7 days. The colonies were then fixed with 4% paraformaldehyde, washed with PBS, and stained with crystal violet. All the assays were performed in triplicate.

2.12 Autophagy analysis

Autophagy was detected using a previously described procedure [24]. Briefly, GFP-LC3 plasmids were transfected into cell

s, which were then treated with trans-gnetin H. The cells were fixed with 4% paraformaldehyde for 30 min and 0.1 M NH4Cl for 10 min and subsequently treated with 0.1% TritonX-100 and incubated with bovine serum albumin. Next, DAPI staining was performed, and the number of GFP-LC3 puncta was counted with a laser confocal microscope.

2.13 Dead cell staining assay

The cytotoxicity of trans-gnetin H was determined using the dead cell staining assay test kit by treating cells with predetermined concentrations of trans-gnetin H for 24 h. Following this, the supernatant was discarded, and the cells was incubated with a working solution of propidium iodide (PI, 8 μM) for 30 min in the dark. The stained cells were then observed and imaged with a fluorescence microscope (OLYMPUS CKX53, Japan).

2.14 Ferroptosis analysis

Cells were grown in 96-well plates until they reached 50%–60% confluence and exposed to different concentrations of RSL3 or erastin (for induction of ferroptosis), in combination with the indicated concentrations of trans-gnetin H. The effect of trans-gnetin H on ferroptosis was determined by assessing cell viability with the CCK8 kit in combination with the Synergy HT microplate reader (Bio-Tek, USA).

2.15 Transmission electron microscopy

H1299 cell pellets were fixed in 2.5% electron microscopy-grade glutaraldehyde in 0.1M sodium cacodylate buffer (pH 7.4) at 4°C overnight. Cell sections were prepared by dehydration, embedding, and curing of the specimens, followed by 50-nm ultrathin section preparation and staining with uranyl acetate and lead citrate. These procedures followed previously described protocols [25]. The ultrathin specimens were examined, and images were acquired with a transmission electron microscope (HT7800, Japan).

2.16 Statistical analysis

The data distribution was assessed using the Shapiro-Wilk test in GraphPad Prism 9.0 for all datasets intended for parametric testing. Homogeneity of variances across groups was tested using Levene's test for all datasets intended for analysis via a one-way or two-way analysis of variance (ANOVA).Data were shown as mean ± SEM. Statistical tests included unpaired one-tailed or two-tailed Student's t-test and one-way or two-way analysis of variance. p value 0.05 was considered statistically significant. In the graphed data *, ** and *** denote p values of < 0.05, 0.01 and 0.001, respectively, ns, not significant.

3. Results

3.1 Trans-gnetin H promotes intracellular ROS generation

We first confirmed its growth-inhibitory effects in these models. Treatment dose-dependently reduced proliferation (Figure 1A, B), with peak efficacy at 10 μM. To dissect the anti-proliferative mechanism, we performed untargeted lipidomics in HT29 cells (10 μM, 2h). PCoA revealed profound metabolic reprogramming (Figure 1C), while volcano plots identified 395 dysregulated metabolites (171 upregulated; 406 downregulated;Figure 1D). KEGG enrichment highlighted glutathione metabolism upregulation (Figure 1E), suggesting oxidative stress.

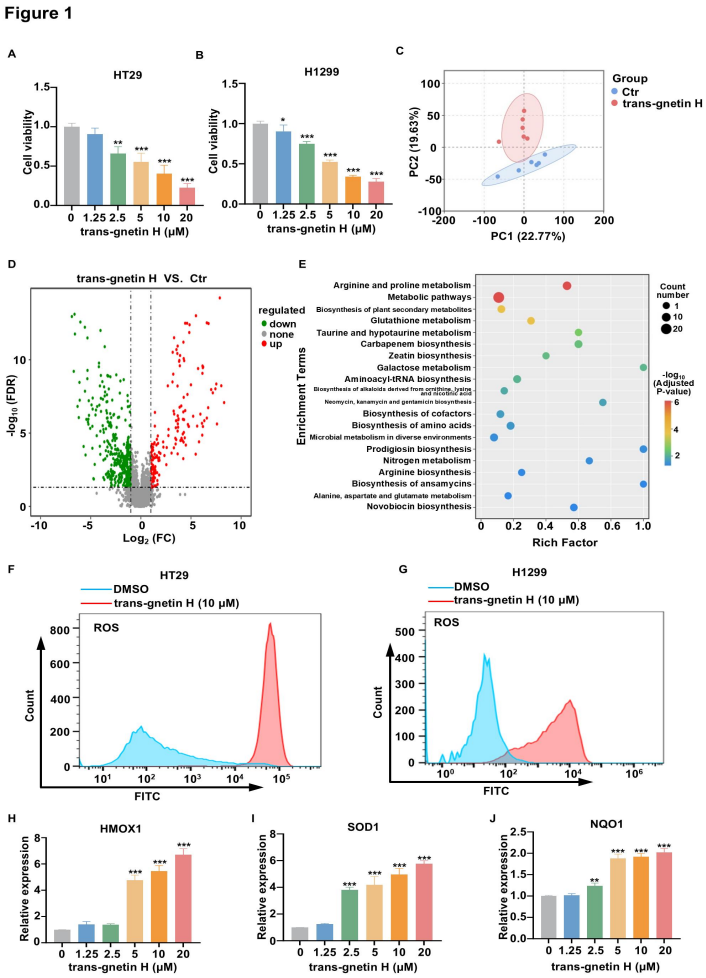

Figure 1. Trans-gnetin H promotes intracellular ROS generation. (A, B) HT29 (A) and H1299 (B) cells were treated with different concentrations of trans-gnetin H for 72 h, the viability of cells was detected by CCK8, n = 3, the number of technical or biological replicates performed. (C-E) Following 2 h treatment with 10 μM trans-gnetin H, HT29 cells from treated and control groups (n=6 per group, equal cell numbers) were collected. Lipids were extracted from each group and analyzed using untargeted liquid chromatography-mass spectrometry (LC-MS) for lipid species identification. (C) Principal component analysis (PCA) score plots distinguish the trans-gnetin H and control groups. (D) The volcano plot reveals 171 significantly upregulated and 406 significantly downregulated metabolites. (E) KEGG pathway analysis was performed on these differential metabolites. (F, G) HT29 (F) and H1299 (G) cells were treated with trans-gnetin H (10 μM) for 2 h, and the ROS levels were detected by FACS. (H-J) HT29 cells were treated with different concentrations of trans-gnetin H for 2 h, and the expression of HMOX1 (H), SOD1 (I), and NQO1 (J) were detected by qRT-PCR. Data were analyzed by one-way ANOVA (A, B, H-J). *p < 0.05, **p < 0.01, ***p< 0.001.

Notably, despite structural similarity to the ROS antagonist resveratrol, trans-gnetin H exhibited opposing redox activity, promp ting our hypothesis of ROS-dependent growth inhibition. Validation studies showed trans-gnetin H significantly increased intrac ellular ROS in both H1299 and HT29 cells (Figure 1F, G). This pro-oxidant effect extended to breast (Figure S1A) and hepatocellu lar carcinoma (Figure S1B) models, suggesting potential broad-spectrum ROS induction across the colon, lung, breast, and hepa tocellular carcinoma. Critically, trans-gnetin H concentration-dependently upregulated antioxidant genes (HMOX1, SOD1, NQO1) , confirming ROS-mediated stress adaptation.

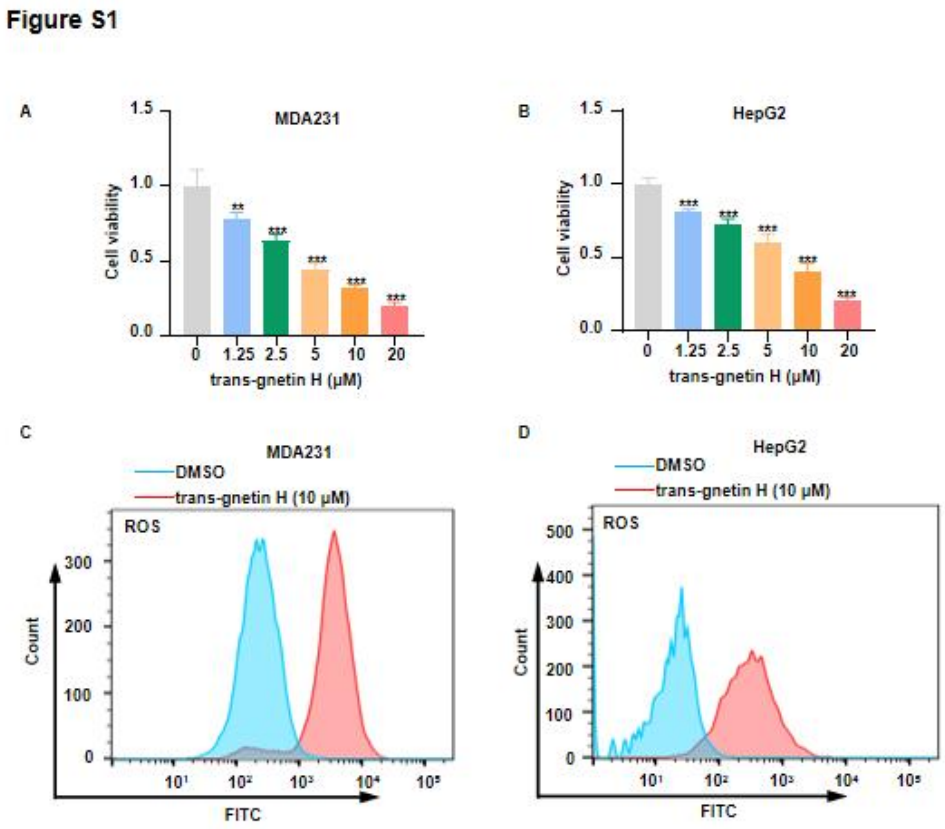

Figure S1. (A, B) MDA231 (A) and HepG2 (B) cells were treated with different concentrations of trans-gnetin H for 72 h, the viability of cells was detected by CCK8, n = 3, the numb er of technical or biological replicates performed. (C,D) MDA231 (C), and HepG2 (D) cells were treated with trans-gnetin H (10 μM) for 2 h, and the ROS levels were detected by FA CS.

3.2 Trans-gnetin H upregulates ROS-associated proteins to suppress mTOR activation

Building upon initial findings, we assessed trans-gnetin H's impact on ROS-regulatory proteins. Treatment concentration-depen dently upregulated both the redox sensor Nrf2 and its effector enzymes HMOX1/SOD1/NQO1 at the protein level (Figure 2A & Figure S2A-D), aligning with prior transcriptional data.

To establish ROS-dependence of Nrf2 induction, we employed ROS scavenger N-acetylcysteine (NAC).NAC co-treatment abolish ed Nrf2 upregulation (Figure 2B & Figure S2B) and attenuated trans-gnetin H-induced expression of HMOX1/SOD1/NQO1 mRN A (Figure 2C-E), with parallel effects on corresponding proteins (Figure 2B& Figure S2E-H).Thus, trans-gnetin H amplifies oxidati ve stress through coordinated Nrf2 pathway activation.

Given established mTORC1 modulation, we examined mTORC2 components. Trans-gnetin H dose-dependently reduced Rictor (mTORC2 core subunit) expression (Figure 2F, G) while suppressing mTORC2-mediated AKT Ser473 phosphorylation [26] and mT ORC1-dependent S6K phosphorylation (Figure 2F, H & Figure S2I-L). Critically, NAC reversed all mTOR-related effects (Figure 2H & Figure S2K, L). Functionally, the mTORC1 activator MHY1485 rescued viability suppression in colony assays (Figure 2I, J). Thes e data establish ROS-mediated dysregulation of both mTOR complexes by trans-gnetin H.

Figure 2

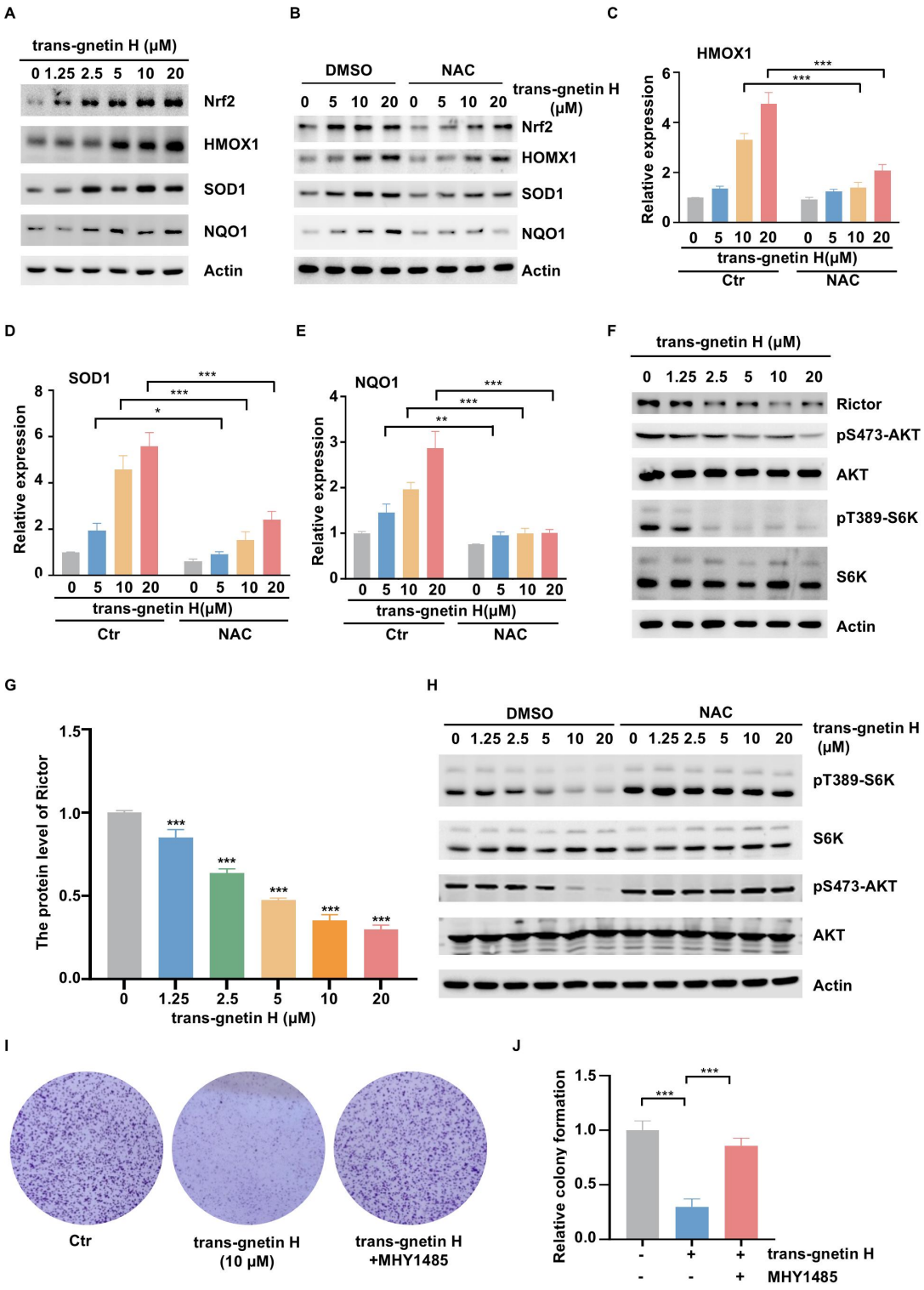

Figure 2. Trans-gnetin H upregulates ROS-associated proteins to suppress mTOR activation. (A) H1299 cells were treated with different concentrations of trans-gnetin H for 2 h, and the indicated proteins were evaluated by western blot. (B) H1299 cells were treated with different concentrations of trans-gnetin H or NAC (2 mM) for 2 h, and the indicated proteins were evaluated by western blot. (C-E) H1299 cells were treated with different concentrations of trans-gnetin H or NAC (2 mM) for 2 h, and then the expression of HMOX1 (C), SOD1 (D), and NQO1 (E) were detected by qRT-PCR. (F, G) HT29 cells were treated with different concentrations of trans-gnetin H for 2 h, and the indicated proteins were evaluated by western blot (F), quantitative for Rictor (G) is presented. (H) H1299 cells were treated with different concentrations of trans-gnetin H or NAC (2 mM) for 2 h, and the indicated proteins were evaluated by western blot. (I, J) HT29 cells were treated with trans-gnetin H (10 μM) or MHY1485 (10 nM), and the cell death was detected by colony formation assay (I), quantitative data are presented in (J).Data were analyzed by one-way ANOVA (G), two-way ANOVA (C-E, J). *p < 0.05, **p < 0.01, ***p< 0.001.

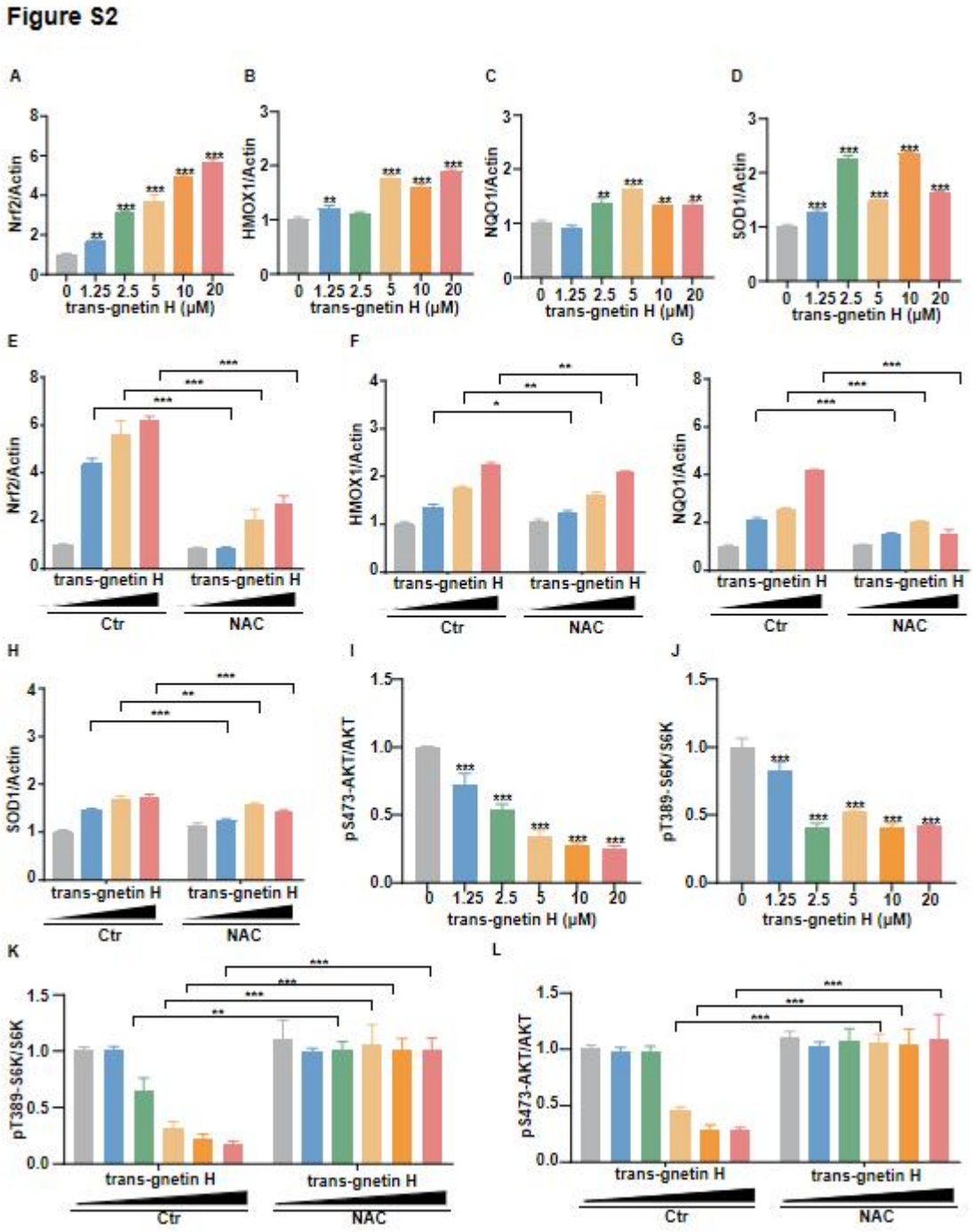

Figure S2. (A-D) H1299 cells were treated with different concentrations of trans-gnetin H for 2 h, and the quantitative results of the detected Nrf2(A) / HMOX1(B) / NQO1(C) / SOD 1(D) protein are shown. (E-H) H1299 cells were treated with different concentrations of trans-gnetin H or NAC (2 mM) for 2 h, and the quantitative results of the detected Nrf2(E) / HMOX1(F) / NQO1(G) / SOD1(H) protein are shown.(I-J) HT29 cells were treated with different concentrations of trans-gnetin H for 2 h, and the quantitative results of the detected pS473-AKT(I) /pT389-S6K(J) protein are shown.(K-L) H1299 cells were treated with different concentrations of trans-gnetin H or NAC (2 mM) for 2 h, and the quantitative results of the detected pT389-S6K protein (K) and pS473-AKT protein (L) are shown. Data were analyzed by one-way ANOVA (A,C), two-way ANOVA (B,D,E). *p < 0.05, **p < 0.01, ***p< 0.001.

3.3 Trans-gnetin H promotes the degradation of Rictor via ROS

We next investigated the mechanism through which trans-gnetin H mediates the decrease in Rictor. However, we found that trans-gnetin H does not regulate Rictor expression at the transcriptional level (Figure 3A). To determine whether trans-gnetin H regulates Rictor at the post-translational level, we treated cells with CHX, an inhibitor of mRNA translation, and found that trans-gnetin H significantly shortens the half-life of Rictor (Figure 3B, C). Numerous previous studies have shown that the half-life of proteins is mainly regulated by ubiquitination [27-29]. Accordingly, our results showed that trans-gnetin H could significantly promote the ubiquitination of Rictor. Moreover, we found that the promotive effect of trans-gnetin H on Rictor

degradation could be blocked by NAC treatment (Figure 3D, E), and the addition of NAC inhibited trans-gnetin-mediated ubiquitination of Rictor (Figure 3F).

It has been shown that ubiquitination of Rictor is mainly regulated by FBXW7α [30]. Therefore, we transfected cells with two siRNAs that specifically target FBXW7α and found that knockdown of FBXW7α blocked trans-gnetin H-mediated Rictor degradation (Figure 3G, H). These results indicate that trans-gnetin H facilitates FBXW7α-mediated ubiquitination of Rictor via ROS, which in turn, promotes Rictor degradation.

Figure 3

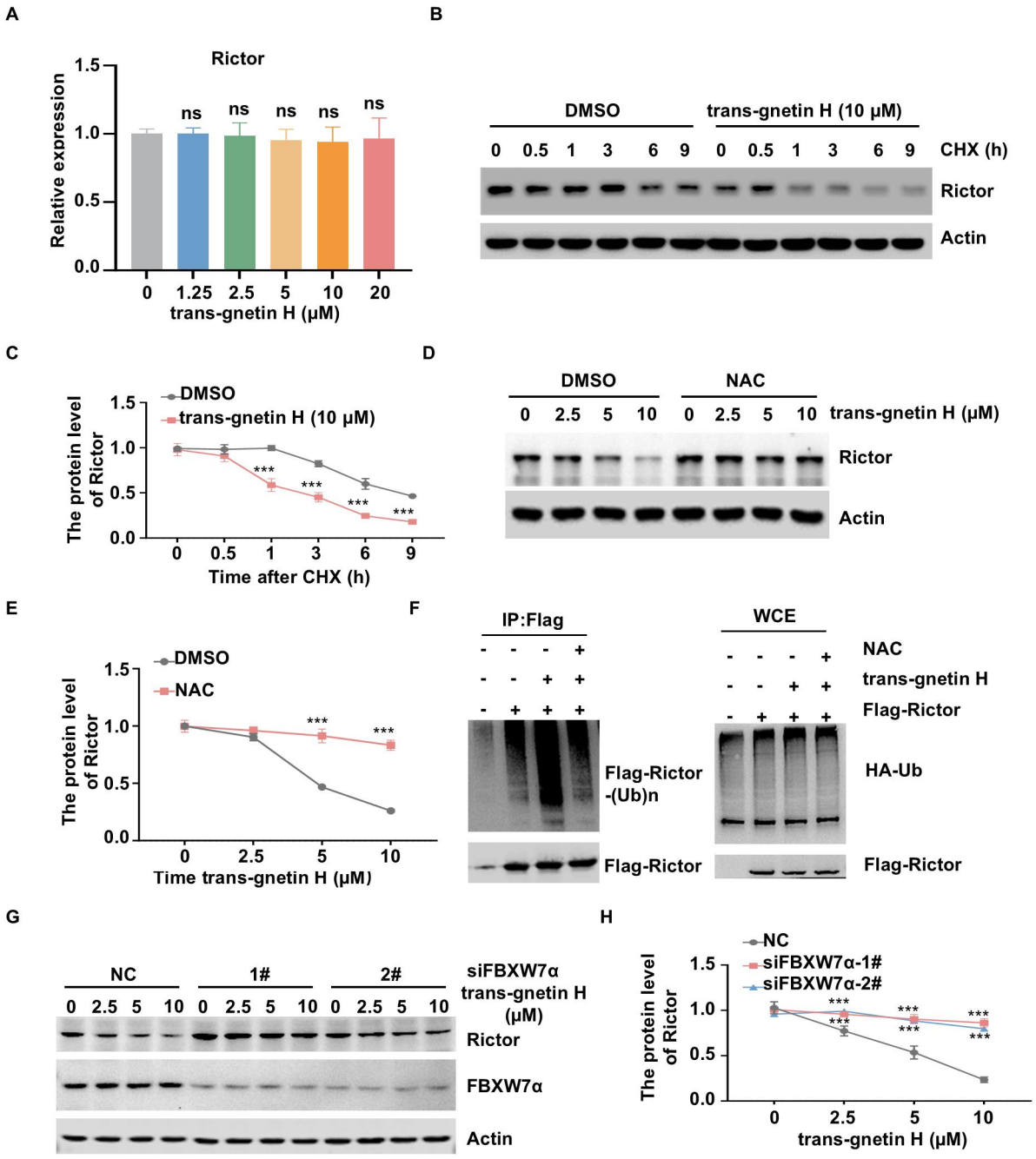

Figure 3. Trans-gnetin H promotes the degradation of Rictor via ROS. (A) HT29 cells were treated with different concentrations of trans-gnetin H for 2 h, and the mRNA of Rictor were evaluated by qRT-PCR. (B, C) HT29 cells were treated with trans-gnetin H (10 μM) or CHX (25 mg/μL) for indicated time, and the indicated proteins were evaluated by western blot (B), quantitative data for Rictor are presented in (C). (D, E) HT29 cells were treated with different concentrations of trans-gnetin H or NAC (2 mM) for 2 h, and the indicated proteins were evaluated by western blot (D), quantitative data for Rictor are presented in (E). (F) HT29 cells were treated with trans-gnetin H (10 μM) or NAC (2 mM) for 2 h, and the Rictor ubiquitination was analyzed by western blot. (G, H) FBXW7α-knockdown HT29 cells were treated with different concentrations of trans-gnetin H for 2 h, and the indicated proteins were evaluated by western blot (G), quantitative data for Rictor are presented in (H). Data were analyzed by one-way ANOVA (A), two-way ANOVA (C, E, H). n = 3, the number of independent experiments performed. *p < 0.05, **p < 0.01, ***p< 0.001.

3.4 Trans-gnetin H does not affect cell ferroptosis

To determine whether trans-gnetin H can regulate cell ferroptosis, we investigated the regulatory effects of trans-gnetin H on li pid ROS production and mitochondrial morphology. Our results demonstrated that trans-gnetin H had no influence on intracell ular lipid ROS generation (Figure 4A, B), even though it significantly promoted ROS generation. Further, trans-gnetin H did not a ffect mitochondrial morphological characteristics either (Figure 4C). In accordance with these results, trans-gnetin H did not pla y a role in sensitivity to erastin (a known inducer of cell ferroptosis) and RSL3-induced ferroptosis (Figure 4D, E). These results s uggest that trans-gnetin H is not involved in cell ferroptosis.

Figure 4

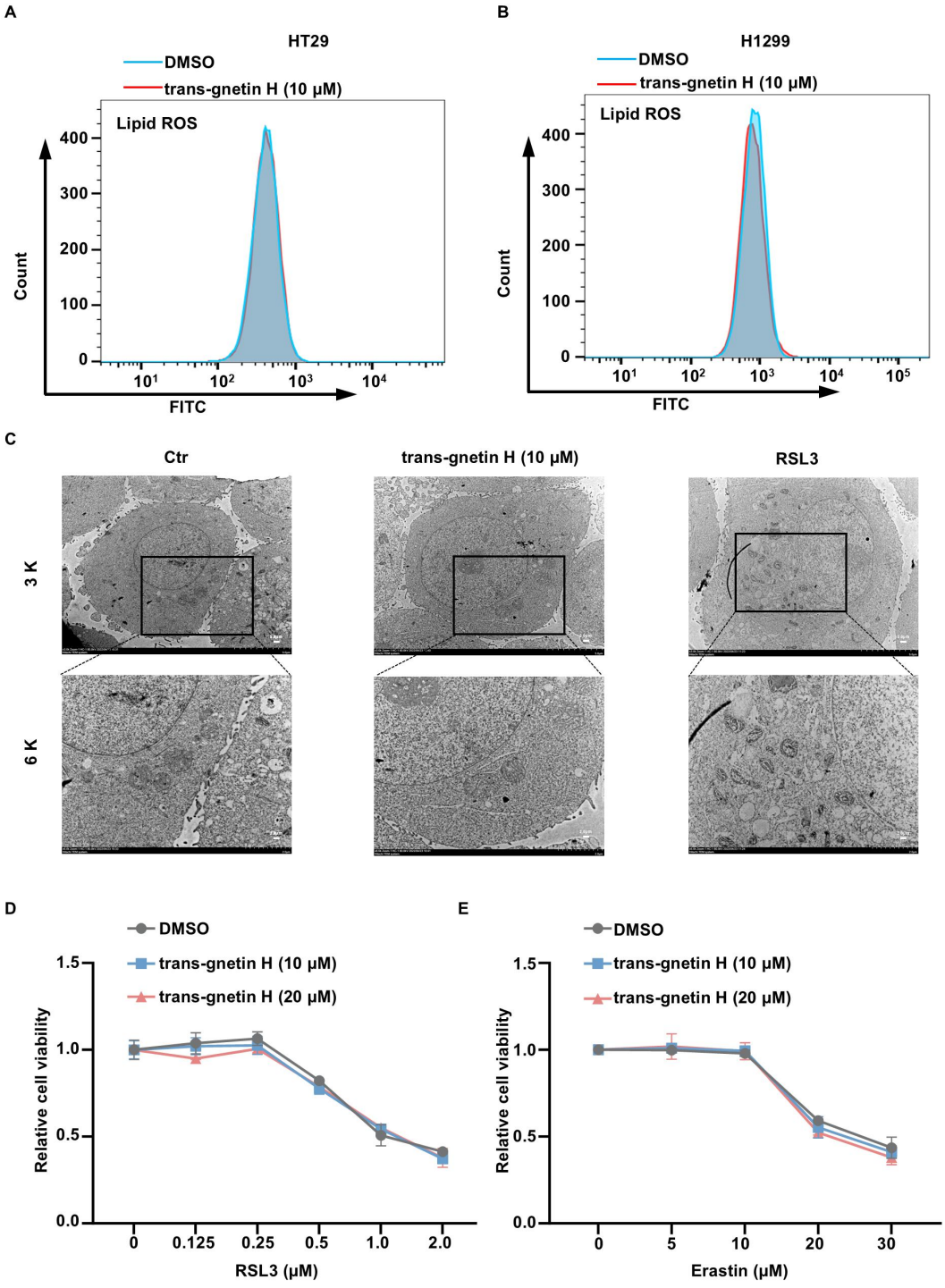

Figure 4. Trans-gnetin H does not affect cell ferroptosis. (A, B) HT29 (A) and H1299 (B) cells were treated with the trans-gnetin H (10 μM) for 2 h, and the lipid ROS was analyzed b y FACS. (C) H1299 cells were treated with the trans-gnetin H (10 μM) or RSL3 (μM) for 12 h, and analyze the ultrastructure of mitochondria with transmission electron microscopy. (D, E) H1299 cells were treated with different concentrations of trans-gnetin H, RSL3 (D) for 24 h or erastin (E) for 24 h, and the viability of indicated cells was examined using CCK8.

3.5 Trans-gnetin H regulates cell viability via ROS

The results of our PI staining experiments on H1299 cells demonstrated that trans-gnetin H significantly inhibited cell growth, and this effect could be blocked by NAC (Figure 5A). Consistent results were obtained with the CCK8 assay (Figure 5B). Moreover, we found that knockdown of FBXW7α blocked the inhibitory effect of trans-gnetin H on cell viability (Figure 5C). In our previous study, we found that trans-gnetin H could regulate cellular autophagy [5]. Consistent with the previous findings, trans-gnetin H demonstrated the ability to significantly promote autophagy (Figure 5D, E). Further, the addition of NAC could block trans-gnetin H-induced autophagy (Figure 5D, E), and knockdown of FBXW7α inhibited the induction of autophagy by trans-gnetin H (Figure 5F, G). Thus, these results suggest that trans-gnetin H has the ability to inhibit cell viability and induce autophagy through pathways that involve ROS and FBXW7α (which mediates ubiquitination of Rictor).

Figure 5

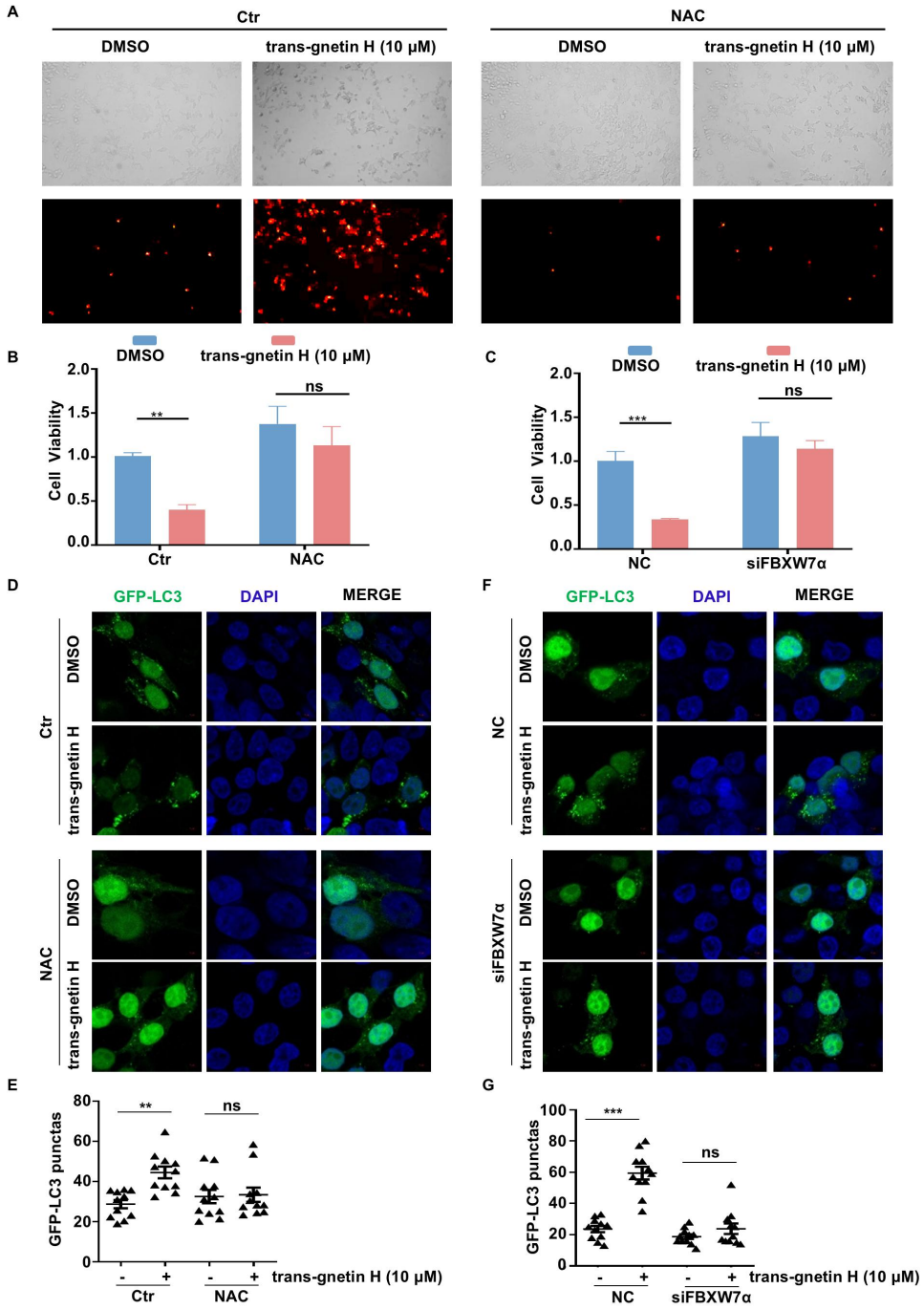

Figure 5. Trans-gnetin H regulates cell viability via ROS. (A) H1299 cells were treated with the trans-gnetin H (10 μM) for 2 h, and the dead cell was detected by staining assay. (B) HT29 cells were treated with the trans-gnetin H (10 μM) or NAC for 2 h, and the cell viability was detected by CCK8. (C) FBXW7α-knockdown HT29 cells were treated with trans-gn

etin H for 2 h, and the cell viability was detected by CCK8. (D, E) HT29 cells were treated with the trans-gnetin H (10 μM) or NAC (2 mM) for 2 h, and autophagy was detected by GFP-LC3 puncta (D), quantitative data for GFP-LC3 puncta are presented in (E). (F, G) FBXW7α-knockdown HT29 cells were treated with trans-gnetin H (10 μM) for 2 h, and autophagy was detected by GFP-LC3 puncta (F), quantitative data for GFP-LC3 puncta are presented in (G). n = 3, the number of technical or biological replicates performed. *p < 0.05, **p < 0.01, ***p< 0.001.

4. Discussion

In the present study, we provide confirmatory evidence for the effect of trans-gnetin H on the cell viability of cancer cells. Further, we demonstrate that the underlying mechanisms involve the inhibition of mTORC1 and mTORC2 activity via the ROS-Rictor signaling axis. Specifically, our results show that trans-gnetin H-induced ROS can regulate mTORC1 activity through the FBXW7α-Rictor-mTORC2-AKT signaling axis: that is, ROS can enhance FBXW7α-mediated ubiquitination and degradation of Rictor, which in turn inhibits mTORC2 and mTORC1 activity. This is a novel mechanism of trans-gnetin H that has not been reported so far, so the findings have significant implications in terms of the future therapeutic potential of trans-gnetin H.

As trans-gnetin H is a trimer of resveratrol, it seems logical that it would have stronger scavenging ability than resveratrol. In contrast, we found that trans-gnetin H promotes the production of cellular ROS and enhances the expression of the Nrf2 protein, which is an important effector protein that plays a role in the response to ROS and is an important indicator of intracellular ROS changes[31]. In addition, we also found the trans-gnetin H upregulates the expression of the downstream Nrf2 antioxidant proteins HMOX1, SOD1, and NQO1. Further, when the cells were pre-treated with NAC before exposure to trans-gnetin H, this effect was inhibited. This suggests that contrary to the previously reported ROS clearance function of resveratrol, trans-gnetin H significantly promotes intracellular ROS production while enhancing intracellular antioxidant protein expression.Thus, although trans-gnetin H is composed of resveratrol, it does not possess all the characteristics of resveratrol.

Resveratrol trimers exhibit a broad spectrum of bioactivities attributed to their structural diversity. Miyabenol C demonstrates notable multi-target pharmacological activities: inducing anti-proliferative and apoptotic effects in tumor cells; inhibiting protein kinase C (PKC); antagonizing the human serotonin (5-HT) receptor; mediating estrogen-like effects via estrogen receptor binding; and exhibiting antagonistic activity toward ecdysone in Drosophila cell models. Significantly, Miyabenol C has been identified as a potent inhibitor of β-secretase (BACE1). It effectively suppresses the pathological production of β-amyloid (Aβ) in both in vitro and in vivo model systems, strongly suggesting its therapeutic potential for central nervous system neurodegenerative disorders such as Alzheimer's disease[32]. Further research revealed that the antitumor effects of another trimer, pauciflorol B, are primarily mediated through activation of the p53 signaling pathway, thereby regulating cellular apoptosis and senescence[33]. In contrast, the trimer α-viniferin displays selective antibacterial activity, exhibiting potent inhibition against Staphylococcus aureus and Escherichia coli, while demonstrating comparatively weaker activity against Salmonella Paratyphi[34]. These examples highlight the functional heterogeneity among resveratrol oligomers and underscore the unique ROS-promoting and mTOR-inhibitory properties of trans-gnetin H identified in our study.

In our next set of experiments, we tried to elucidate the potential mechanism underlying intracellular ROS production induced by trans-gnetin H. First, we tried to detect changes in the function of the four complexes in the mitochondrial respiratory chain, but we found that trans-gnetin H did not affect this mechanism of ROS production. Studies have shown that lipid overload-induced toxicity and insulin resistance is one of the mechanisms that drives ROS production, and cholesterol and oxidized sterols can also cause mitochondrial dysfunction and ROS production[35]. However, our non-targeted lipidomics analysis of trans-gnetin H-treated cells showed that there was no increase in cholesterol and fatty acids after trans-gnetin H treatment. Thus, the mitochondrial and lipid overload mechanisms of intracellular ROS production were ruled out as the ROS induction pathways of trans-gnetin H.

We next analyzed the molecular structure of trans-gnetin H and found a large number of hydroxyl groups (-OH). Based on this observation, we speculated that hydroxyl radicals released from trans-gnetin H may account for the increase in ROS observed in cells treated with trans-gnetin H. In addition, we analyzed the phenotype at the cellular level, and our results showed that the expression of superoxide dismutase and catalase was significantly inhibited by trans-gnetin H. Superoxide dismutase binds to the superoxide by-products of oxidative phosphorylation and converts them to hydrogen peroxide and diatomic oxygen. Thus, changes in these enzymes may also be an important factor in the promotion of ROS production by trans-gnetin H.

In our previous studies, trans-gnetin H was found to inhibit mTORC1 activity by activating the AMPK pathway[5]. In this study, we also wanted to explore whether trans-gnetin H has an effect on mTORC2. Our results show that trans-gnetin H significantly suppressed the phosphorylation of AKT at Ser473, which is a conserved site for mTORC2-mediated phosphorylation on AKT[26]. Thus, our results suggest that trans-gnetin H can also significantly inhibit mTORC2 activity. We wanted to learn more about how trans-gnetin H performs this function. Our previous study showed that vitamin C-induced ROS regulated mTORC2 activation by promoting the degradation of Rictor[36], which is an important component protein of mTORC2 [37]. Building upon these findings, we further investigated the effect of trans-gnetin H on Rictor. Our data demonstrate that trans-gnetin H inhibits mTORC2 activity by inducing intracellular ROS generation, which activates the ubiquitin ligase FBXW7α. This activation triggers ubiquitination and subsequent proteasomal degradation of the mTORC2 component Rictor. Notably, although trans-gnetin H potently induced FBXW7α-mediated Rictor ubiquitination and degradation, it failed to enhance the FBXW7α-Rictor physical interaction in co-immunoprecipitation assays (Figure S3A). This finding suggests that

trans-gnetin H/ROS facilitates Rictor ubiquitination through mechanisms independent of strengthening the FBXW7α-Rictor binding affinity. While this dissociation between binding affinity and degradation efficiency warrants further investigation, it is well-established that mTORC2 regulates mTORC1 activity via AKT phosphorylation at Ser473. This established link aligns with our prior observation of trans-gnetin H-mediated mTORC1 inhibition. Therefore, collectively, our findings indicate that trans-gnetin H suppresses mTORC1 activity through dual pathways: AMPK activation and mTORC2 inhibition.

Figure S3

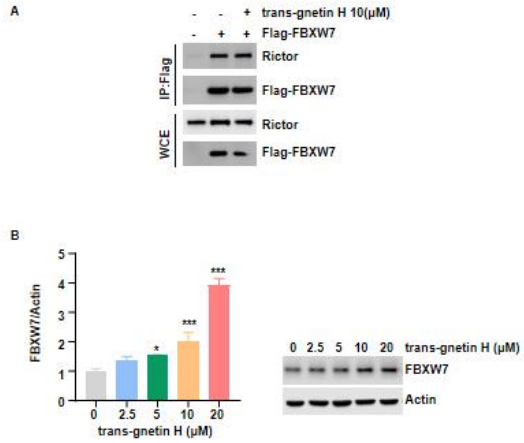

Figure S3. (A) Flag-FBXW7 was overexpressed in HT29 cells and the cells were treated with trans-gnetin H (10 μM) for 2 h, the interaction between Flag-FBXW7 and Rictor was detected by Co-IP assay. (B) HT29 cells were treated with different concentrations of trans-gnetin H for 2 h, and the quantitative results of the detected FBXW7 protein are shown.

Further supporting this proposed mechanism, our supplementary experiments revealed that trans-gnetin H significantly upregulates FBXW7 protein expression (Figure S3B). This finding indicates that trans-gnetin H not only facilitates FBXW7-mediated ubiquitination and degradation of Rictor but may also potentiate FBXW7's regulatory effect on Rictor by directly enhancing FBXW7 expression. Within cellular systems, FBXW7 exists as three distinct isoforms: the α isoform localizes predominantly to the nucleus, the β isoform exhibits cytoplasmic distribution, and the γ isoform primarily resides within the nucleolus[38]. Given this broad subcellular distribution of FBXW7, examining only its subcellular localization may be insufficient to elucidate the precise mechanism by which trans-gnetin H or ROS regulate FBXW7-mediated Rictor degradation. It is extensively documented that GSK3β-mediated phosphorylation of Rictor triggers FBXW7-dependent degradation[30]. Although this study did not directly assess FBXW7 phosphorylation status, our functional analyses demonstrate that trans-gnetin H-induced ROS promotes Rictor degradation specifically through FBXW7α—highlighting a central finding of this work. Therefore, post-translational modifications (PTMs) of FBXW7α, such as phosphorylation, represent a plausible regulatory mechanism through which ROS may modulate its activity, constituting a significant direction for future investigations.

Autophagy is a highly conserved self-degrading system induced primarily by nutritional deprivation or stress[35]. It contributes to the maintenance of cellular homeostasis by promoting the degradation of intracellular protein aggregates, organelles, and other macromolecules [39]. Abnormalities in autophagy may induce the initiation phase of tumorigenesis. In the later stages of tumor development, autophagy is essential for obtaining nutrients and dealing with the unfavorable tumor microenvironment [40]. Our previous study showed that trans-gnetin H can promote autophagy via inhibition of the mTORC1-TFEB signaling axis to facilitate the localization of TFEB within the nucleus [5]. TFEB belongs to a class of transcription factors that have been reported to regulate lysosomal biogenesis and autophagic gene expression [41]. In the present study, we have expanded on the related mechanisms by reporting that trans-gnetin H-promoted autophagy is highly dependent on ROS. Further, we found that the promotive effect of ROS on autophagy was brough about via suppression of the mTOR pathway. By combining our present findings with our previous findings, we can deduce that trans-gnetin H promotes autophagy through the mTOR/AMPK/ROS axis. In the future, it would be interesting to explore the mechanisms involved as a way of identifying potential treatment targets.

Elevated ROS is an important feature of cell ferroptosis, and lipid ROS and mitochondrial crinkling represent the gold standard for detecting cell ferroptosis [42]. In this study, we tried to find evidence that trans-gnetin H regulates ferroptosis in cells. As shown in Figure 4, although trans-gnetin H did result in a significant increase in the generation of intracellular ROS and had a broad spectrum of other effects, it did not induce the production of intracellular lipid ROS (elevated lipid ROS is an important condition for ferroptosis). In addition, our experimental results show that trans-gnetin H has no obvious destructive effect on the mitochondria in the cell. Importantly, our ferroptosis assay showed that trans-gnetin H did not cause ferroptosis in cells. In line with the present findings, in our previous study, too, we ruled out the ability of trans-gnetin H to cause apoptosis. In summary, we believe that the production of intracellular ROS induced by trans-gnetin H inhibits the activity of mTOR and activates autophagy, similar to our previous study.

In this paragraph, we will highlight some of the questions that are still to be answered in the future and some limitations of our study. The selection of cancer cell lines in this study was strategically aligned with global cancer burden data. The four cell lines investigated—NCI-H1299 (lung cancer), HT29 (colorectal cancer), HepG2 (liver cancer), and MDA-MB-231 (breast cancer)—represent malignancies ranked highest in global incidence and mortality: lung cancer ranks first in mortality, colorectal cancer third in incidence, liver cancer second in mortality, and breast cancer first in incidence[43]. These cancers collectively span major physiological systems (respiratory, digestive, and reproductive), enhancing the translational relevance of our findings across diverse human cancers.However, it is important to note that while our initial screening included MDA-MB-231 and HepG2 cells, our subsequent detailed mechanistic investigations focused primarily on H1299 and HT29

models. Consequently, the generalizability of the specific RO S-Rictor-mTOR signaling axis identified in this study to breast cancer (MDA-MB-231) and liver cancer (HepG2) cells remains to be fully characterized and constitutes a limitation of this work. Additionally, the experiments were conducted at the c ellular level and need to be verified through in vivo studies in the future, especially for evaluating the side effects of trans-gnetin H.our cellular models inherently overlook tumor micr oenvironment complexity and interpatient heterogeneity wit hin each cancer type. For instance, while MDA-MB-231 repre sents triple-negative breast cancer, other molecular subtypes (e.g., HER2+, ER+) may respond differently[44]. Similarly, the reliance on single cell lines per cancer type limits extrapolati on to intratumoral genomic diversity. Future studies incorpor ating primary patient-derived cells, co-culture systems, and i n vivo models will be essential to confirm pathophysiological relevance. At the level of mechanism analysis, our previous s tudy showed that mTORC1 can be inhibited by trans-gnetin H [5], and in our present study, trans-gnetin H was found to ha ve the ability to inhibit both mTORC1 and mTORC2 activity vi a ROS, as well as the viability of the cancer cell lines examine d. While these findings indicate the potential anti-tumor effe cts of trans-gnetin H, it is not clear which upstream signaling molecule of mTOR is targeted by trans-gnetin H-induced ROS. Current studies on the upstream signaling molecules of mTO RC1 focus on amino acids, growth factors, and glucose [45], s o they might shed light on the potential targets of trans-gneti n H-induced ROS. In the future, this line of investigation migh t help identify therapeutic targets for cancer treatment. In ou r previous study, we also found that trans-gnetin H inhibited mTORC1 activity through AMPK [5], but in this study, we did not investigate the relationship between ROS and the AMPK pathway. Thus, it is not clear whether ROS can regulate mTO R through the AMPK pathway, or whether the regulation of t he ROS-FBXW7α-Rictor axis is dependent on AMPK signaling. Another limitation was that although we found that ROS can promote FBXW7α-mediated ubiquitination and degradation of Rictor, we did not clarify the mechanism of ROS regulation of FBXW7α. Thus, whether ROS promotes the expression of FBXW7α or regulates its stability is a topic that warrants inve stigating. Another shortcoming of the present study is that w e have not explored whether trans-gnetin H can cause pyropt osis and necrotic apoptosis, which is a topic we hope to expl ore in subsequent studies.

In summary, the present findings reveal that trans-gnetin H i nhibits tumor cell viability through the following pathway: tr ans-gnetin H-induced increase in ROS production leads to FB XW7α-mediated ubiquitination degradation of Rictor; this fur ther leads to inhibition of mTORC2 activity that, in turn, inhib its mTORC1 activity via inhibition of AKT phosphorylation. Wi th regard to the underlying mechanism, we were able to add to the literature by demonstrating that trans-gnetin H can re gulate cell viability and autophagy through its effects on ROS and FBXW7α.

References

[1] C. Lennicke, H.M. Cocheme, Redox metabolism: ROS as specific molecular regulators of cell signaling and function, Mol Cell 81(18) (2021) 3691-3707.

[2] B. Singla, R. Holmdahl, G. Csanyi, Editorial: Oxidants and Redox Signaling in Inflammation, Front Immunol 10 (2019) 545.

[3] D.D. Roberts, Extracellular Matrix and Redox Signaling in Cellular Responses to Stress, Antioxid Redox Signal 27(12) (2017) 771-773.

[4] C.K. Sen, S. Roy, Redox signals in wound healing, Biochim Biophys Acta 1780(11) (2008) 1348-61.

[5] C. Xia, G. Wang, L. Chen, H. Geng, J. Yao, Z. Bai, L. Deng, Trans-gnetin H isolated from the seeds of Paeonia species induces autophagy via inhibiting mTORC1 signalling through AMPK activation, Cell Prolif (2022) e13360.

[6] Y. Gao, C. He, R. Ran, D. Zhang, D. Li, P.G. Xiao, E. Altman, The resveratrol oligomers, cis- and trans-gnetin H, from Paeonia suffruticosa seeds inhibit the growth of several human cancer cell lines, J Ethnopharmacol 169 (2015) 24-33.

[7] J. Zhang, K. Ma, T. Qi, X. Wei, Q. Zhang, G. Li, J.F. Chiu, P62 regulates resveratrol-mediated Fas/Cav-1 complex formation and transition from autophagy to apoptosis, Oncotarget 6(2) (2015) 789-801.

[8] C.H. Chang, C.Y. Lee, C.C. Lu, F.J. Tsai, Y.M. Hsu, J.W. Tsao, Y.N. Juan, H.Y. Chiu, J.S. Yang, C.C. Wang, Resveratrol-induced autophagy and apoptosis in cisplatin-resistant human oral cancer CAR cells: A key role of AMPK and Akt/mTOR signaling, Int J Oncol 50(3) (2017) 873-882.

[9] Y. Qin, Z. Ma, X. Dang, W. Li, Q. Ma, Effect of resveratrol on proliferation and apoptosis of human pancreatic cancer MIA PaCa-2 cells may involve inhibition of the Hedgehog signaling pathway, Mol Med Rep 10(5) (2014) 2563-7.

[10] J.Y. Jang, E. Im, N.D. Kim, Mechanism of Resveratrol-Induced Programmed Cell Death and New Drug Discovery against Cancer: A Review, Int J Mol Sci 23(22) (2022).

[11] J. Yang, X. Zhou, X. Zeng, O. Hu, L. Yi, M. Mi, Resveratrol attenuates oxidative injury in human umbilical vein endothelial cells through regulating mitochondrial fusion via TyrRS-PARP1 pathway, Nutr Metab (Lond) 16 (2019) 9.

[12] C. Tan, H. Zhou, X. Wang, K. Mai, G. He, Resveratrol attenuates oxidative stress and inflammatory response in turbot fed with soybean meal based diet, Fish Shellfish Immunol 91 (2019) 130-135.

[13] K. Szkudelska, M. Okulicz, I. Hertig, T. Szkudelski, Resveratrol ameliorates inflammatory and oxidative stress in type 2 diabetic Goto-Kakizaki rats, Biomed Pharmacother 125 (2020) 110026.

[14] S.C. Chao, Y.J. Chen, K.H. Huang, K.L. Kuo, T.H. Yang, K.Y. Huang, C.C. Wang, C.H. Tang, R.S. Yang, S.H. Liu, Induction of sirtuin-1 signaling by resveratrol induces human chondrosarcoma cell apoptosis and exhibits antitumor activity, Sci Rep 7(1) (2017) 3180.

[15] Z. Liu, X. Wu, J. Lv, H. Sun, F. Zhou, Resveratrol induces p53 in colorectal cancer through SET7/9, Oncol Lett 17(4) (2019) 3783-3789.

[16] S.H. Lee, Y.J. Lee, Synergistic anticancer activity of resveratrol in combination with docetaxel in prostate carcinoma cells, Nutr Res Pract 15(1) (2021) 12-25.

[17] S. Battaglioni, D. Benjamin, M. Wälchli, T. Maier, M.N. Hall, mTOR substrate phosphorylation in growth control, Cell 185(11) (2022) 1814-1836.

[18] G. Wang, L. Chen, S. Qin, T. Zhang, J. Yao, Y. Yi, L. Deng, Mechanistic Target of Rapamycin Complex 1: From a Nutrient Sensor to a Key Regulator of Metabolism and Health, Adv Nutr 13(5) (2022) 1882-1900.

[19] Y.K. He, X.T. Cen, S.S. Liu, H.D. Lu, C.N. He, Protective effects of ten oligostilbenes from Paeonia suffruticosa seeds on interleukin-1β-induced rabbit osteoarthritis chondrocytes, BMC Chem 13(1) (2019) 72.

[20] V. Matyash, G. Liebisch, T.V. Kurzchalia, A. Shevchenko, D. Schwudke, Lipid extraction by methyl-tert-butyl ether for high-throughput lipidomics, J Lipid Res 49 (2008) 1137–1146.

[21] M. Holcapek, G. Liebisch, K. Ekroos, Lipidomic analysis, Anal Bioanal Chem 90 (2020) 4249–4257.

[22] C.Wang, Y. Tong, Y. Wen, J. Cai, H. Guo, L. Huang, Hepatocellular carcinoma-associated protein td26 interacts and enhances sterol regulatory element-binding protein 1 activity to promote tumor cell proliferation and growth, Hepatology 68 (2018) 1833–1850.

[23] G. Wang, S. Qin, Y. Zheng, C. Xia, P. Zhang, L. Zhang, J. Yao, Y. Yi, L. Deng, T-2 Toxin Induces Ferroptosis by Increasing Lipid Reactive Oxygen Species (ROS) and Downregulating Solute Carrier Family 7 Member 11 (SLC7A11), J Agric Food Chem 69(51) (2021) 15716-15727.

[24] L. Deng, C. Jiang, L. Chen, J. Jin, J. Wei, L. Zhao, M. Chen, W. Pan, Y. Xu, H. Chu, X. Wang, X. Ge, D. Li, L. Liao, M. Liu, L. Li, P. Wang, The ubiquitination of rag A GTPase by RNF152 negatively regulates mTORC1 activation, Mol Cell 58(5) (2015) 804-818.

[25] H. Lee, F. Zandkarimi, Y. Zhang, J.K. Meena, J. Kim, L. Zhuang, S. Tyagi, L. Ma, T.F. Westbrook, G.R. Steinberg, D. Nakada, B.R. Stockwell, B. Gan, Energy-stress-mediated AMPK activation inhibits ferroptosis, Nat Cell Biol 22(2) (2020) 225-234.

[26] D.D. Sarbassov, D.A. Guertin, S.M. Ali, D.M. Sabatini, Phosphorylation and regulation of Akt/PKB by the rictor-mTOR complex, Science 307(5712) (2005) 1098-101.

[27] L. Deng, T. Meng, L. Chen, W. Wei, P. Wang, The role of ubiquitination in tumorigenesis and targeted drug discovery, Signal Transduct Target Ther 5(1) (2020) 11.

[28] S. Bae, S.Y. Kim, J.H. Jung, Y. Yoon, H.J. Cha, H. Lee, K. Kim, J. Kim, I.S. An, J. Kim, H.D. Um, I.C. Park, S.J. Lee, S.Y. Nam, Y.W. Jin, J.H. Lee, S. An, Akt is negatively regulated by the MULAN E3 ligase, Cell Res 22(5) (2012) 873-85.

[29] J.H. Mao, I.J. Kim, D. Wu, J. Climent, H.C. Kang, R. DelRosario, A. Balmain, FBXW7 targets mTOR for degradation and cooperates with PTEN in tumor suppression, Science 321(5895) (2008) 1499-502.

[30] J. Koo, X. Wu, Z. Mao, F.R. Khuri, S.Y. Sun, Rictor Undergoes Glycogen Synthase Kinase 3 (GSK3)-dependent, FBXW7-mediated Ubiquitination and Proteasomal Degradation, J Biol Chem 290(22) (2015) 14120-9.

[31] A.T. Dinkova-Kostova, I.M. Copple, Advances and challenges in therapeutic targeting of NRF2, Trends Pharmacol Sci (2023).

[32] J. Hu, T. Lin, Y. Gao, J. Xu, C. Jiang, G. Wang, G. Bu, H. Xu, H. Chen, Y. Zhang, The resveratrol trimer miyabenol C inhibits β-secretase activity and β-amyloid generation, PLoS One 10(1) (2015) e0115973.

[33] H. Qiao, X. Chen, L. Xu, J. Wang, G. Zhao, Y. Hou, H. Ge, R. Tan, E. Li, Antitumor effects of naturally occurring oligomeric resveratrol derivatives, FASEB J 27(11) (2013) 4561-71.

[34] W. Zain, N. Ahmat, N. Norizan, N. Nazri, The evaluation of antioxidant, antibacterial and structural identification activity of trimer resveratrol from Malaysia's dipterocarpaceae, J Basic Appl Sci (2011) 926–929.

[35] N. Mizushima, M. Komatsu, Autophagy: renovation of cells and tissues, Cell 147(4) (2011) 728-41.

[36] S. Qin, G. Wang, L. Chen, H. Geng, Y. Zheng, C. Xia, S. Wu, J. Yao, L. Deng, Pharmacological vitamin C inhibits mTOR signaling and tumor growth by degrading Rictor and inducing HMOX1 expression, Plos Genet 19(2) (2023) e1010629.

[37] D.D. Sarbassov, S.M. Ali, D.H. Kim, D.A. Guertin, R.R. Latek, H. Erdjument-Bromage, P. Tempst, D.M. Sabatini, Rictor, a novel binding partner of mTOR, defines a rapamycin-insensitive and raptor-independent pathway that regulates the cytoskeleton, Curr Biol 14(14) (2004) 1296-302.

[38] M. Welcker, B. Clurman, FBW7 ubiquitin ligase: a tumour suppressor at the crossroads of cell division, growth and differentiation, Nat Rev Cancer 8(2) (2008) 83-93.

[39] Y. Xu, X. Yang, Autophagy and pluripotency: self-eating your way to eternal youth, Trends Cell Biol 32(10) (2022) 868-882.

[40] H. Yamamoto, S. Zhang, N. Mizushima, Autophagy genes in biology and disease, Nat Rev Genet (2023) 1-19.

[41] H. Yang, J.X. Tan, Lysosomal quality control: molecular mechanisms and therapeutic implications, Trends Cell Biol (2023).

[42] B.R. Stockwell, Ferroptosis turns 10: Emerging mechanisms, physiological functions, and therapeutic applications, Cell 185(14) (2022) 2401-2421.

[43] H. Sung, J. Ferlay, R. Siegel, M. Laversanne, I. Soerjomataram, A. Jemal, F. Bray, Global cancer statistics 2020: GLOBOCAN estimates of incidence and mortality worldwide for 36 cancers in 185 countries, CA Cancer J Clin 71(3) (2021) 209-249.

[44] Y. Li, J. Duan, X. Bian, S. Yu, Triple-negative breast cancer molecular subtyping and treatment progress, Breast Cancer Res 22 (1) (2020).

[45] R. Shams, Y. Ito, H. Miyatake, Mapping of mTOR drug targets: Featured platforms for anti-cancer drug discovery, Pharmacol Ther 232 (2022) 108012.

Author Contributions：Shiyang Lou: Conceptualization, Methodology, Writing—original draft, Investigation. **Ruixu Zhang:** Methodology, Writing—original draft, Investigation. **Chao Xia**: Methodology, Writing—original draft, Investigation. **Yining Zheng:** Methodology, Investigation**. Miaomiao Zhu:** Methodology, Investigation. **Dingping Feng:** Methodology, Investigation. **Lu Deng:** Conceptualization, Methodology, Writing—original draft, Investigation, Writing—review and editing, Resources, Supervision, Project administration and Funding acquisition.

Funding information： The authors gratefully thank professor Pu Liu (Henan University of Science and Technology) for the help of compounds isolation and the members of the professor Junhu Yao lab for their assistance. This work was financially supported by the Shenzhen Municipal Basic Research Program (Natural Science Foundation) General Program Project (Grant No. JCYJ20240813152007010);National Natural Science Foundation of China - General Program Project (Grant No. 82472705).**Conflict of interest statement：** The authors declare that they have no conflict of interest.**Data Availability Statement：** The data that support the findings of this study are available from the corresponding author upon reasonable request.**Ethical statement：** We promise that the results of this study will be reported in an honest, objective, and responsible manner without any modification or manipulation that may mislead the reader or compromise the integrity of the study.